electronics

MDPI

Article

On the Trade-Off between Energy Efficiency and Spectral Efficiency in RIS-Aided Multi-User MISO Downlink

Meng Zhang [1], Le Tan [1], Kelin Huang [1] and Li You [2,*]

[1] School of Information Science and Engineering, Southeast University, Nanjing 211189, China; 213183594@seu.edu.cn (M.Z.); 213180077@seu.edu.cn (L.T.); 213180320@seu.edu.cn (K.H.)
[2] National Mobile Communications Research Laboratory, Southeast University, Nanjing 210096, China
* Correspondence: liyou@seu.edu.cn

Abstract: As reconfigurable intelligent surfaces (RISs) have been gradually brought to reality, a large amount of research has been conducted to investigate the immense benefits of RISs. That is because RISs enable us to artificially direct the radio wave propagating through the environment at a relatively low cost. This paper investigates the trade-off between spectral efficiency (SE) and energy efficiency (EE) in the RIS-aided multi-user multiple-input single-output downlink. We develop an optimization framework for designing the transmitting precoding at the base station and the phase shift values at the RIS to balance the EE-SE trade-off. The proposed iterative optimization framework for the design includes quadratic transform, alternating optimization, and weighted minimization mean-square error conversion. Simulation results illustrate our optimization framework algorithm exhibits effectiveness and a fast convergence rate.

Keywords: energy efficiency; intelligent reflecting surface (IRS); multi-user downlink; reconfigurable intelligent surface (RIS); spectral efficiency

Citation: Zhang, M.; Tan, L.; Huang, K.; You, L. On the Trade-Off Between Energy Efficiency and Spectral Efficiency in RIS-Aided Multi-User MISO Downlink. *Electronics* **2021**, *10*, 1307. https://doi.org/10.3390/electronics10111307

Academic Editors: Dinh-Thuan Do, Alagan Anpalagan, Fatemeh Afghah and Evangelos Pallis

Received: 22 April 2021
Accepted: 26 May 2021
Published: 30 May 2021

1. Introduction

As increasingly more 5G technology is being brought from concept to reality, the era of 5G has already started. A concept named reconfigurable intelligent surface (RIS) is proposed to achieve a higher data rate and increased availability and soon became a hot research topic. In practice, RIS is an artificial radio structure composed of low-cost units which can be programmed to reflect incoming radio-frequency waves to specified directions [1]. What makes RIS unique as a part of the environment is that it can control its reaction to the impinging radio wave by changing the inside current compared to the conventional surface [2,3]. According to the physical laws, the traditional surface, such as a wall, has a fixed reflection characteristic. As RIS can adapt to time-varying wireless communication environments, it makes the concept of intelligent radio environments possible [3]. The propagation environments become reconfigurable by adding RISs into the wireless environments. The process of installing RISs on or removing RISs from walls or ceilings has a low implementation cost as the hardware footprints are relatively low [4–7]. Therefore, RIS is expected to be the cost-efficient and energy-saving technology to improve system performance, becoming one of the hot topics in future communication networks [8–11].

Through the research of channel modeling [12,13], channel estimation [14], and performance evaluation of the communication system based on the RIS [15–17], the potential benefits of the communication environments based on RIS are discussed. In the resource allocation design of RIS-aided communication, large amounts of work focus on optimizing the spectral efficiency (SE) of the system [18]. Furthermore, we treat energy efficiency (EE), which is another important topic in the research on RIS [19,20], as one of the optimization objectives. However, most of the existing work has focused on the optimization of either SE or EE. SE performance is sometimes sacrificed for the maximization of EE, especially

when the value of Signal to Interference plus Noise Ratio (SINR) is large [21,22]. Therefore, we try to find a way to attain a balance between EE and SE.

In this paper, a trade-off between SE and EE is investigated while the transmitting precoding at the base station (BS) side and the phase shift values at the RIS of RIS-aided multi-user multiple-input single-output (MISO) downlink are jointly optimized. The main contributions made by this paper are listed as follows.

We consider a RIS-aided multiuser downlink system to attain an EE-SE trade-off. Next, we propose an optimization framework for the problem in joint optimization. Then, we develop an optimization algorithm to design the transmitting precoding at the BS side and the phase shift values at the RIS to attain this trade-off. We first use the alternating optimization (AO) method to decouple the optimization variables. We also use quadratic transform and weighted minimization mean-square error (WMMSE) to turn the problem into a strictly convex problem.

The rest of this article is organized as follows. We introduce the optimization problem of the RIS-aided multiuser MISO downlink system in Section 2. Then, we present an algorithm framework to handle the problem in Section 3. In Section 4, we present further numerical analysis according to simulation results. At last, we provide the conclusion of this paper in Section 5.

Notation 1. *We use* $\mathbf{A}$ *to denote a matrix, while* $a_{i,j}$ *and* $\mathbf{a}_k$ *denote the* (i,j)*-th element and the* k*-th column vector of matrix* $\mathbf{A}$*, respectively. We also use* $\mathbf{x}$ *to denote a column vector, while* x_i *and* $\|\mathbf{x}\|$ *denote the* i*-th element and the Euclidean norm of vector* $\mathbf{x}$*, respectively. An* $M \times M$ *identity matrix is denoted by* $\mathbf{I}_M$ *in this paper. The notation* $|b|$ *denotes the modulus value of complex scalar* b*. The operator* $\mathsf{diag}\{\cdot\}$ *is used as the diagonalization operator in this paper. We use* $\mathcal{CN}(\mathbf{a}, \mathbf{B})$ *to denote Circular symmetric complex Gaussian distribution. The conjugate, argument, and real part of a complex number* Φ *are denoted by* Φ^**,* $\angle\Phi$*, and* $\Re\{\Phi\}$*, respectively.*

2. System Model and Problem Formulation

2.1. Channel Model

The paper considers a multiuser MISO downlink communication based on RIS, as shown in Figure 1. The messages are sent from one M-antenna BS to K users, and each user is equipped with a single antenna. The RIS in the system is equipped with N reflection elements to form a new communication path from the BS to the K users. We use $\mathbf{h}_{\mathrm{d},k} \in \mathbb{C}^{M\times 1}$, $\mathbf{G} \in \mathbb{C}^{M\times N}$, and $\mathbf{h}_{\mathrm{r},k} \in \mathbb{C}^{N\times 1}$, $k = 1, \ldots, K$, to denote the channel vectors from the BS to user k, from the BS to RIS, and from RIS to user k, respectively.

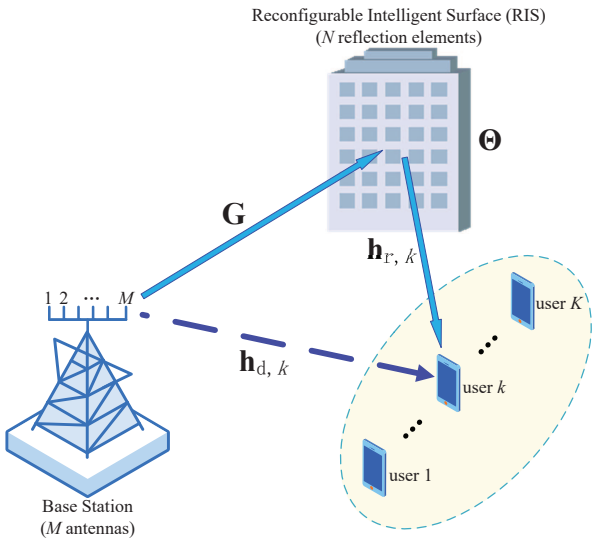

Figure 1. The reconfigurable intelligent surface (RIS)-aided multi-user multiple-input single-output (MISO) downlink system.

The reflection operation, which is finished by the N RIS elements, directed by an intelligent controller in RIS, will change the incident signal by multiplying it with $\theta_n \in \mathcal{F}$, where $\mathcal{F}$ refers to the feasible set of reflection coefficient (RC).The RIS will then forward this composite signal just like transmitting it from a point source [15].

Moreover, only the first-time-reflected signals are considered in the communication model considering substantially high path loss [18,23]. We use a diagonal matrix $\mathbf{\Theta} = \sqrt{\eta}\,\mathrm{diag}(\theta_1, \ldots, \theta_n, \ldots, \theta_N)$, where $\eta \leq 1$ indicates the reflection efficiency, to denote the RIS phase-shift operation.

2.2. Signal Model

We can express the transmitted signal at the BS as

$$\mathbf{x} = \sum_{k=1}^{K} \mathbf{w}_k s_k \tag{1}$$

where $\mathbf{w}_k \in \mathbb{C}^{M\times 1}$ is used to denote corresponding transmit precoding vector, while s_k denotes the transmit message to user k. It is assumed that s_k, $k = 1, \ldots, K$, are independent random variables with zero mean and unit variance. Then, we use y_k to denote the signal received by user k. The expression of y_k is given below. Note that the difference between the two paths is usually negligible as the RIS is usually placed close to the transmitter or receiver to get minimal path loss. Otherwise, it needs to conduct an estimation of the delay at the BS [5,24] and phase compensation at the receiver when the difference between the two propagation delays gets large [25].

$$\begin{aligned} y_k &= \underbrace{\mathbf{h}_{\mathrm{d},k}^H \mathbf{x}}_{\text{Direct link}} + \underbrace{\mathbf{h}_{\mathrm{r},k}^H \mathbf{\Theta}^H \mathbf{G}^H \mathbf{x}}_{\text{RIS}-\text{aided link}} + u_k \\ &= (\mathbf{h}_{\mathrm{d},k}^H + \mathbf{h}_{\mathrm{r},k}^H \mathbf{\Theta}^H \mathbf{G}^H) \sum_{k=1}^{K} \mathbf{w}_k s_k + u_k \end{aligned} \tag{2}$$

where $u_k \sim \mathcal{CN}(0, \sigma_0^2)$ refers to the additive white Gaussian noise (AWGN) in the channel [26].

2.3. Problem Formulation

All the signals from other users (i.e., $s_1, \ldots, s_{k-1}, s_{k+1}, \ldots, s_K$) are treated as interference by the k-th user. Therefore, the decoding SINR of s_k can be expressed as

$$\gamma_k = \frac{\left|(\mathbf{h}_{\mathrm{d},k}^H + \mathbf{h}_{\mathrm{r},k}^H \mathbf{\Theta}^H \mathbf{G}^H)\mathbf{w}_k\right|^2}{\sum_{i=1, i\neq k}^{K} \left|(\mathbf{h}_{\mathrm{d},k}^H + \mathbf{h}_{\mathrm{r},k}^H \mathbf{\Theta}^H \mathbf{G}^H)\mathbf{w}_i\right|^2 + \sigma_0^2}. \tag{3}$$

According to Equation (3), EE and SE of this RIS-aided downlink communication system can be expressed as

$$\mathrm{EE} = \frac{\sum_{k=1}^{K} \omega_k \log(1+\gamma_k)}{\mu \sum_{k=1}^{K} \|\mathbf{w}_k\|^2 + P_{\mathrm{s,total}}} \tag{4a}$$

$$\mathrm{SE} = \sum_{k=1}^{K} \omega_k \log(1+\gamma_k) \tag{4b}$$

where μ is the reciprocal of the transmit power amplifier efficiency, and ω_k refers to the weight in the SE of the system given to k-th user. In Equation (4a), the term $P_{\mathrm{s,total}} = P_{\mathrm{BS}} + NP_n + KP_k$ is the sum of the static hardware power consumed by the BS, the RIS, and the users. It refers to the fixed power consumed by the system [5]. Let $\mathbf{W} = [\mathbf{w}_1, \mathbf{w}_2, \ldots, \mathbf{w}_K] \in \mathbb{C}^{M\times K}$. Thus, we can get the joint optimization problem below.

$$\text{(P1)} \quad \max_{\mathbf{W},\boldsymbol{\Theta}} \; a\frac{\sum_{k=1}^{K}\omega_k \log(1+\gamma_k)}{\mu\sum_{k=1}^{K}\|\mathbf{w}_k\|^2 + P_{\text{s,total}}} + (1-a)\sum_{k=1}^{K}\omega_k \log(1+\gamma_k) \tag{5a}$$

$$\text{s.t.} \; \sum_{k=1}^{K}||\mathbf{w}_k||^2 \le \mathrm{P_T} \tag{5b}$$

$$\theta_n \in \mathcal{F}, \; \forall n = 1, \cdots, N \tag{5c}$$

where a refers to the weight of EE, $0 < a < 1$, and (5b) refers to the constraint on the transmit power at the BS side. In this paper, $\mathcal{F}$ is chosen as the continuous phase set [4,27–29], which means that $\|\theta_n\|^2 = 1$. Therefore, $\mathcal{F}$ can be expressed as

$$\mathcal{F} = \{\theta_n \mid \theta_n = e^{j\phi_n}, \; \phi_n \in [0, 2\pi)\}. \tag{6}$$

The problem in (5a) is non-convex with the fractional expression of EE, and it is harder than the problem that only chooses SE as the objective. This paper tries to optimize the objective in problem (P1) with low computational complexity.

3. Joint Optimization of EE-SE

3.1. Quadratic Transform

As the fractional expression in the problem brings difficulties in designing an algorithm, we can get the equivalently transformed expression of (P1) by applying the quadratic transform in [30]. Therefore, we change the fractional problem into a new form without the fraction to simplify the optimization problem. The new problem is expressed as

$$\begin{aligned}\text{(P2)} \quad \max_{\mathbf{W},\boldsymbol{\Theta},y} \; & 2y\sqrt{a\sum_{k=1}^{K}\omega_k \log(1+\gamma_k)} \\ & - y^2\left(\mu\sum_{k=1}^{K}\|\mathbf{w}_k\|^2 + P_{\text{s,total}}\right) \\ & + (1-a)\sum_{k=1}^{K}\omega_k \log(1+\gamma_k) \\ \text{s.t.} \; & \text{(5b)}, \text{(5c)}\end{aligned} \tag{7}$$

where $y \in \mathbb{R}$ is an auxiliary variable brought by the quadratic transform algorithm.

Next, the square root of the SE part contained in the objective function in problem (P2) is replaced with variable t. Furthermore, a new constraint on t needs to be added to ensure that the problem is reformulated equivalently.

$$\begin{aligned}\text{(P3)} \quad \max_{\mathbf{W},\boldsymbol{\Theta},y,t} \; & 2y\sqrt{a}\,t - y^2\left(\mu\sum_{k=1}^{K}\|\mathbf{w}_k\|^2 + P_{\text{s,total}}\right) \\ & + (1-a)\sum_{k=1}^{K}\omega_k \log(1+\gamma_k) \\ \text{s.t.} \; & \text{(5b)}, \text{(5c)} \\ & t^2 \le \sum_{k=1}^{K}\omega_k \log(1+\gamma_k)\end{aligned} \tag{8}$$

Therefore, optimizing the objective in problem (P1) over $\mathbf{W}$ and $\boldsymbol{\Theta}$ is equivalently turned to the process of finding the optimal $\mathbf{W}$, $\boldsymbol{\Theta}$, y, and t for the problem (P3). As the problem (P3) makes it difficult to find the optimal values of the four variables simultaneously, the AO method is then adopted to conduct the optimization by organizing the original problem into several sub-problems. The iteration step is repeated until the convergence is reached. First and foremost, y and t are optimized, while the algorithm to optimize $\boldsymbol{\Theta}$ and $\mathbf{W}$ alternately will be introduced in Section 3.2. During the process of optimizing the objective over y and t, we can have

$$t^{\text{opt}} = \sqrt{\sum_{k=1}^{K} \omega_k \log(1+\gamma_k)} \tag{9a}$$

$$y^{\text{opt}} = \frac{\sqrt{a \sum_{k=1}^{K} \omega_k \log(1+\gamma_k)}}{\mu \sum_{k=1}^{K} \|\mathbf{w}_k\|^2 + P_{\text{s,total}}}. \tag{9b}$$

By setting the derivative of the target function in (P3) to zero, the expression of y^{opt} can be obtained. The objective function in (P1) appears after substituting y^{opt} and t^{opt} for y and t in problem (P3), which also proves that problem (P3) is equivalent to problem (P1).

3.2. WMMSE Algorithm

When optimizing $\boldsymbol{\Theta}$ and $\mathbf{W}$ for problem (P3), we first focus on optimizing the latter part, which refers to the weighted sum-rate term, in problem (P3). Therefore, we obtain the new problem as

$$\begin{aligned} \text{(P4)} \quad & \max_{\mathbf{W},\boldsymbol{\Theta}} \sum_{k=1}^{K} \omega_k \log(1+\gamma_k) \\ & \text{s.t. } (5b), (5c). \end{aligned} \tag{10}$$

As problem (P4) is also non-convex, it is still hard to conduct the optimization. According to the work in [31], the WMMSE algorithm can be applied to optimize the SE of the system. We can equivalently transform problem (P4) into a convex optimization problem by introducing two auxiliary variables, while we can get the closed-form expression of the optimal solutions for these two variables. The equivalently formed problem is

$$\begin{aligned} \text{(P5)} \quad & \min_{\mathbf{W},\boldsymbol{\Theta},\mathbf{u},\boldsymbol{\alpha}} \sum_{k=1}^{K} \omega_k(\alpha_k e_k - \log \alpha_k) \\ & \text{s.t. } (5b), (5c) \end{aligned} \tag{11}$$

where $\mathbf{u} \in \mathbb{C}^{K\times 1}$, $\boldsymbol{\alpha} \in \mathbb{R}^{K\times 1}$, and e_k are auxiliary variables introduced by the algorithm. The first two variables $\mathbf{u}$ and $\boldsymbol{\alpha}$ refer to $[u_1, \ldots, u_K]^T$ and $[\alpha_1, \ldots, \alpha_K]^T$, respectively. The rest variable e_k is expressed as

$$\begin{aligned} e_k =& |u_k^* \left(\mathbf{h}_{\text{d},k}^H + \mathbf{h}_{\text{r},k}^H \boldsymbol{\Theta}^H \mathbf{G}^H\right) \mathbf{w}_k - 1|^2 \\ & + \sum_{i=1, i\neq k}^{K} \left| u_i \left(\mathbf{h}_{\text{d},k}^H + \mathbf{h}_{\text{r},k}^H \boldsymbol{\Theta}^H \mathbf{G}^H\right) \mathbf{w}_i \right|^2 + \sigma_0^2 |u_k|^2. \end{aligned} \tag{12}$$

When optimizing $\boldsymbol{\Theta}$ and $\mathbf{W}$ for problem (P3), we can remove some irrelevant items. With the equivalence relation between problems (P4) and (P5), we can turn problem (P3) into

$$\begin{aligned} \text{(P6)} \quad & \min_{\mathbf{W},\boldsymbol{\Theta},\mathbf{u},\boldsymbol{\alpha}} y^2 \left(\mu \sum_{k=1}^{K} \|\mathbf{w}_k\|^2 + P_{\text{s,total}}\right) + (1-a) \sum_{k=1}^{K} \omega_k(\alpha_k e_k - \log \alpha_k) \\ & \text{s.t.} \quad (5b), (5c). \end{aligned} \tag{13}$$

Next, we will alternately optimize $\mathbf{W}$, $\boldsymbol{\Theta}$, $\mathbf{u}$, and $\boldsymbol{\alpha}$ for problem (P6). The optimization of $\boldsymbol{\Theta}$ and $\mathbf{W}$ will be introduced in the following, while the optimal u_k and α_k are obtained by setting the derivatives to zero, respectively:

$$u_k^{\text{opt}} = \frac{\left(\mathbf{h}_{\text{d},k}^H + \mathbf{h}_{\text{r},k}^H \boldsymbol{\Theta}^H \mathbf{G}^H\right) \mathbf{w}_k}{\sum_{i=1}^{K} \left| \left(\mathbf{h}_{\text{d},k}^H + \mathbf{h}_{\text{r},k}^H \boldsymbol{\Theta}^H \mathbf{G}^H\right) \mathbf{w}_i \right|^2 + \sigma_0^2} \tag{14a}$$

$$\alpha_k^{\text{opt}} = \frac{1}{e_k} \tag{14b}$$

where $k = 1, 2, \cdots, K$.

3.2.1. Optimization of Transmit Precoding for Given Phase-Shifting Values

To optimize the objective in problem (P6) over $\mathbf{W}$, we remove the terms that are independent of $\mathbf{W}$ and get

$$\begin{aligned} (\text{P7}) \quad & \min_{\mathbf{W}} \; y^2\mu \textstyle\sum_{k=1}^{K} ||\mathbf{w}_k||^2 + (1-a) \sum_{k=1}^{K} \omega_k \alpha_k e_k \\ & \text{s.t. } (5\text{b}). \end{aligned} \tag{15}$$

Then, we rewrite e_k as below. Therefore, we can rewrite the objective function and transform problem (P7) equivalently into new problem (P7) below.

$$\begin{aligned} e_k &= |u_k^* \mathbf{h}_k^H \mathbf{w}_k - 1|^2 + \sum_{i=1, i\neq k}^{K} \left| u_i \mathbf{h}_k^H \mathbf{w}_i \right|^2 + \sigma_0^2 |u_k|^2 \\ &= \sum_{i=1}^{K} |u_i|^2 \mathbf{w}_i^H \mathbf{h}_k \mathbf{h}_k^H \mathbf{w}_i - 2\Re\{u_k \mathbf{w}_k^H \mathbf{h}_k\} + 1 + \sigma_0^2 |u_k|^2 \end{aligned} \tag{16}$$

$$\begin{aligned} (\text{P7}) \quad & \min_{\mathbf{W}} \; \textstyle\sum_{k=1}^{K} \mathbf{w}_k^H (y^2\mu \mathrm{I}_M + (1-a)|u_k|^2 \sum_{i=1}^{K} \omega_i \alpha_i \mathbf{h}_i \mathbf{h}_i^H) \mathbf{w}_k \\ & \quad - 2\Re\Big\{ (1-a)\omega_k \alpha_k u_k \mathbf{w}_k^H \mathbf{h}_k \Big\} + (1-a)\omega_k \alpha_k (1 + \sigma_0^2 |u_k|^2) \\ & \text{s.t.} \quad (5\text{b}) \end{aligned} \tag{17}$$

where $\mathbf{h}_i = \mathbf{h}_{\mathrm{d},i} + \mathbf{G}\boldsymbol{\Theta}\mathbf{h}_{\mathrm{r},i}$ and I_M denotes an $M \times M$ identity matrix.

Considering that $\mu > 0$, $(1-a) > 0$, $\omega_i \geq 0$, $\alpha_i > 0$, new problem (P7) is convex. Then, we can use standard convex optimization algorithms [32] to find the optimal value of $\mathbf{W}$.

3.2.2. Optimization of Phase-Shifting Values for Given Transmitting Precoding

To optimize problem (P6) over $\boldsymbol{\Theta}$, the terms which do not correlate with $\boldsymbol{\Theta}$ can be omitted, and new problem forms as

$$\begin{aligned} (\text{P8}) \quad & \min_{\boldsymbol{\Theta}} \; \textstyle\sum_{k=1}^{K} \omega_k \alpha_k e_k \\ & \text{s.t. } (5\text{c}). \end{aligned} \tag{18}$$

As variable $\boldsymbol{\Theta}$ is a diagonal matrix, we can transform the variable of problem (P8) into vector $\boldsymbol{\theta}$ through some substitution and operation and rewrite the objective function in problem (P8) in the quadratic form of $\boldsymbol{\theta}$. Therefore, we add some auxiliary variables $\mathbf{a}_{i,k} = \sqrt{\eta}\,\mathrm{diag}(\mathbf{h}_{\mathrm{r},k}^H)\mathbf{G}^H \mathbf{w}_i$ and $b_{i,k} = \mathbf{h}_{\mathrm{d},k}^H \mathbf{w}_i$. Thus, we have $\left(\mathbf{h}_{\mathrm{d},k}^H + \mathbf{h}_{\mathrm{r},k}^H \boldsymbol{\Theta}^H \mathbf{G}^H\right)\mathbf{w}_i = b_{i,k} + \boldsymbol{\theta}^H \mathbf{a}_{i,k}$, where $\boldsymbol{\theta} = [\theta_1, \ldots, \theta_N]^T$ [26]. Then, we can transform e_k into the new form below to simplify the expression of the optimization problem. Therefore, we can rewrite the objective function in (18), and problem (P8) can be equivalently expressed as new problem (P8) below.

$$\begin{aligned} e_k &= |u_k^* (\mathrm{b}_{k,k} + \boldsymbol{\theta}^H \mathbf{a}_{k,k}) - 1|^2 + \sum_{i=1, i\neq k}^{K} \left| u_i (\mathrm{b}_{i,k} + \boldsymbol{\theta}^H \mathbf{a}_{i,k}) \right|^2 + \sigma_0^2 |u_k|^2 \\ &= \boldsymbol{\theta}^H \left(\sum_{i=1}^{K} |u_i|^2 \mathbf{a}_{i,k} \mathbf{a}_{i,k}^H \right) \boldsymbol{\theta} + 2\Re\left\{ \boldsymbol{\theta}^H \left(\sum_{i=1}^{K} |u_i|^2 \mathrm{b}_{i,k}^* \mathbf{a}_{i,k} - u_k^* \mathbf{a}_{k,k} \right) \right\} \\ &\quad + \left(\sum_{i=1}^{K} |u_i|^2 |\mathrm{b}_{i,k}|^2 - 2\Re\{u_k^* \mathrm{b}_{k,k}\} + \sigma_0^2 |u_k|^2 + 1 \right) \end{aligned} \tag{19}$$

$$\begin{aligned} (\text{P8}) \quad & \min_{\boldsymbol{\theta}} \ \boldsymbol{\theta}^H \mathbf{U} \boldsymbol{\theta} + 2\Re\{\boldsymbol{\theta}^H \mathbf{v}\} + \mathrm{C} \\ & \text{s.t. } (5\text{c}) \end{aligned} \tag{20}$$

where

$$\mathbf{U} = \sum_{k=1}^{K} \omega_k \alpha_k \left(\sum_{i=1}^{K} |u_i|^2 \mathbf{a}_{i,k} \mathbf{a}_{i,k}^H\right) \tag{21a}$$

$$\mathbf{v} = \sum_{k=1}^{K} \omega_k \alpha_k \left(\sum_{i=1}^{K} |u_i|^2 b_{i,k}^* \mathbf{a}_{i,k} - u_k^* \mathbf{a}_{k,k}\right) \tag{21b}$$

$$\mathrm{C} = \sum_{k=1}^{K} \omega_k \alpha_k \left(\sum_{i=1}^{K} |u_i|^2 |\mathrm{b}_{i,k}|^2 - 2\Re\left\{u_k^* \mathrm{b}_{k,k}\right\} + \sigma_0^2 |u_k|^2 + 1\right). \tag{21c}$$

Next, we change the variable $\boldsymbol{\Theta}$ into $\boldsymbol{\theta}$ to conduct the optimization of new problem (P8). Then, we optimize the new problem (P8) over $\theta_1, \ldots, \theta_N$ in turn [26]. While conducting the optimization over one variable θ_n, $n = 1, \ldots, N$, the values of θ_j $(j = 1, \ldots, N, j \neq n)$ are fixed. In addition, the $\boldsymbol{\theta}^H \mathbf{U} \boldsymbol{\theta}$ and $\boldsymbol{\theta}^H \mathbf{v}$ in the new problem (P8) can be transformed as

$$\begin{aligned} \boldsymbol{\theta}^H \mathbf{U} \boldsymbol{\theta} &= \sum_{i=1}^{N} \sum_{j=1}^{N} \theta_i^* \mathrm{u}_{i,j} \theta_j \\ &= \theta_n^* \mathrm{u}_{n,n} \theta_n + 2\Re\left\{\sum_{j=1, j\neq n}^{\mathrm{N}} \theta_n^* \mathrm{u}_{n,j} \theta_j\right\} \\ &\quad + \sum_{i=1, i\neq n}^{N} \sum_{j=1, j\neq n}^{N} \theta_i^* \mathrm{u}_{i,j} \theta_j \end{aligned} \tag{22a}$$

$$\boldsymbol{\theta}^H \mathbf{v} = \theta_n^* \mathrm{v_n} + \sum_{i=1, i\neq n}^{N} \theta_i^* \mathrm{v}_i. \tag{22b}$$

Then, we need to conduct the optimization over θ_n. Therefore, the expression of problem (P8) can be adapted to the optimization problem below by removing the unrelated items.

$$\begin{aligned} (\text{P9}) \quad & \min_{\theta_n} \ \theta_n^* \mathrm{u}_{n,n} \theta_n + 2\Re\left\{\theta_n^* \left(\mathrm{v}_n + \sum_{j=1, j\neq n}^{N} \mathrm{u}_{n,j} \theta_j\right)\right\} \\ & \text{s.t. } \theta_n = \mathrm{e}^{\jmath \phi_n}, \ \phi_n \in [0, 2\pi). \end{aligned} \tag{23}$$

The value of the first part of the objective function is independent of θ_n, so only the second part of the expression is needed to be considered while doing the optimization as $\theta_n = \mathrm{e}^{\jmath \phi_n}$. It can be easily seen that

$$\phi_n^{\mathrm{opt}} = \pi + \angle\left(\mathrm{v}_n + \sum_{j=1, j\neq n}^{N} \mathrm{u}_{n,j} \theta_j\right) \tag{24}$$

where $n = 1, 2, \cdots, N$.

So far, we have managed to propose a complete framework for problem (P1) with low complexity. We first introduce auxiliary variable y by using the quadratic transform and replace the square root term with variable t, combining with the corresponding constraint, to turn the original problem into problem (P3) equivalently. Then, we use the AO method to decouple the optimization variables while optimizing the objective in the new problem. When optimizing the objective function in problem (P3), we use the WMMSE transform to turn problem (P3) into a convex problem. Then, we can use standard convex optimization algorithms [32] to find the solution.

4. Numerical Results

In this section, we will provide some simulation results to evaluate the performance of the framework for the trade-off of the EE and SE. During the simulation, we use the 3GPP spatial channel model under the suburban macro-cell propagation scenario [33,34]. The adopted parameters during the simulation are shown in the Table 1 below for clarity [35].

Table 1. Simulation setup parameters.

Parameters	Values
Path loss	-110 dB
Number of users K	4
Weight for each user in the system's SE	$\frac{1}{K}$
Number of RIS reflecting units N	8
Number of BS antennas M	4
The reciprocal of the power amplifier efficiency at the BS μ	5
The reflection efficiency of the RIS η	0.8
The noise variance at the users σ_0^2	-130 dBm
Static power consumption of each user P_k	10 dBm
Hardware dissipated power at the BS P_{BS}	40 dBm
Per-element static power at the RIS P_n	20 dBm

The average convergence performance of the proposed algorithm is illustrated in Figure 2. The result demonstrates that the convergence is achieved with a small number of iterations.

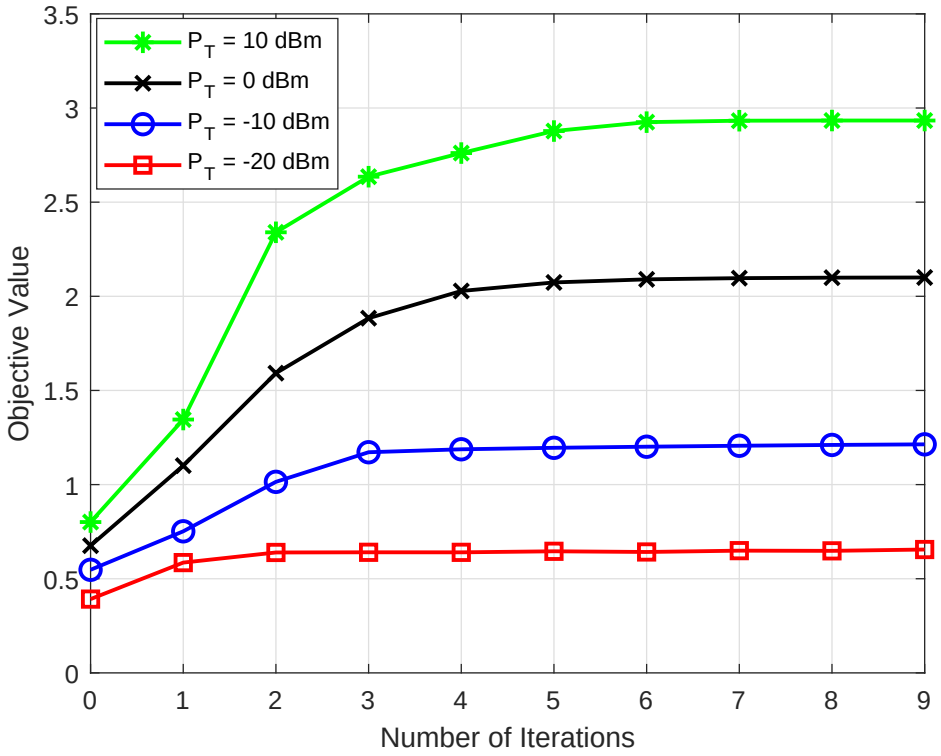

Figure 2. Average convergence performances versus the number of iterations for $a = 0.5$.

The EE-SE trade-off curves attained by the algorithm framework under different values of BS power constraint P_{T} and weight a are shown in Figure 3. Obviously, EE-SE trade-offs under different weighting factors are similar to each other when the value of P_{T} is small, approximately when $P_{\mathrm{T}} < 20$ dBm, as all available power of BS can be fully utilized and both EE and SE are maximized when P_{T} is small. Therefore, changes in values of a have little impact on the EE-SE trade-off when P_{T} is small. When P_{T} gets high, the EE-SE trade-offs under different a differ greatly. It is observed that the increasing of a brings about an increase in EE optimization and a decrease in SE, and the decreasing of a causes a decrease in EE and an increase in SE. That is because larger weight is given to EE for larger a, and thus more focus is transferred to EE when conducting the optimization. However, more focus is transferred to the SE optimization when a smaller weight is given to EE for smaller a.

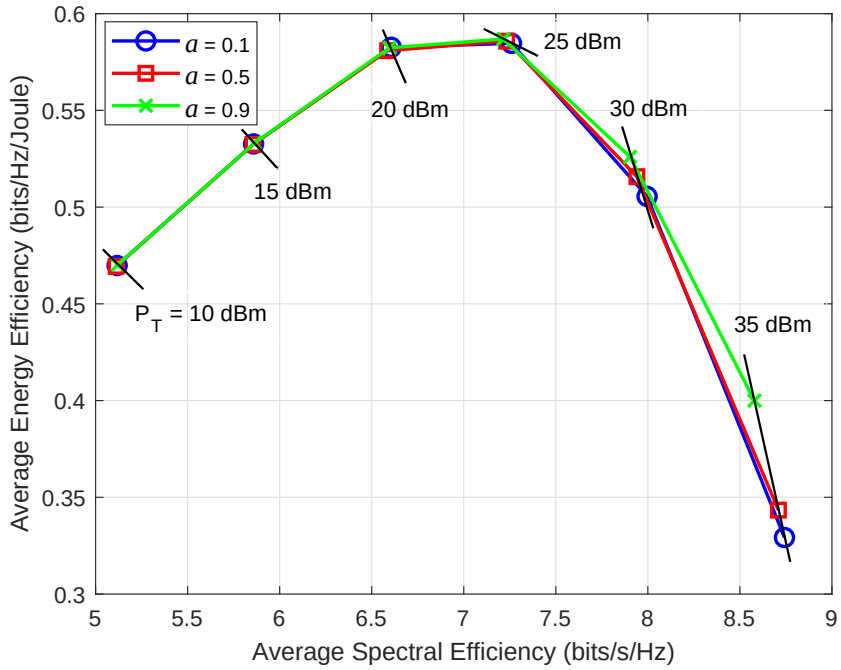

Figure 3. Average EE-SE trade-offs with different a under different transmit power budgets P_{T}.

In Figure 4, we show the EE-SE trade-offs of the system under the condition of $a = 0.5$. In order to illustrate the necessity of jointly optimizing the transmit precoding matrix and the phase shift values for optimizing the system SE and EE, the results of the EE-SE trade-off is provided in a baseline case. In the baseline, the phase shift values at the RIS are given randomly and are not optimized. It can also be observed that under the same transmission power constraint P_{T} of the BS, the EE and SE results of the joint optimization are greater than those of the baseline, respectively. It indicates that jointly optimizing the transmit precoding matrix and the phase shift values is beneficial for improving the SE and EE of the system.

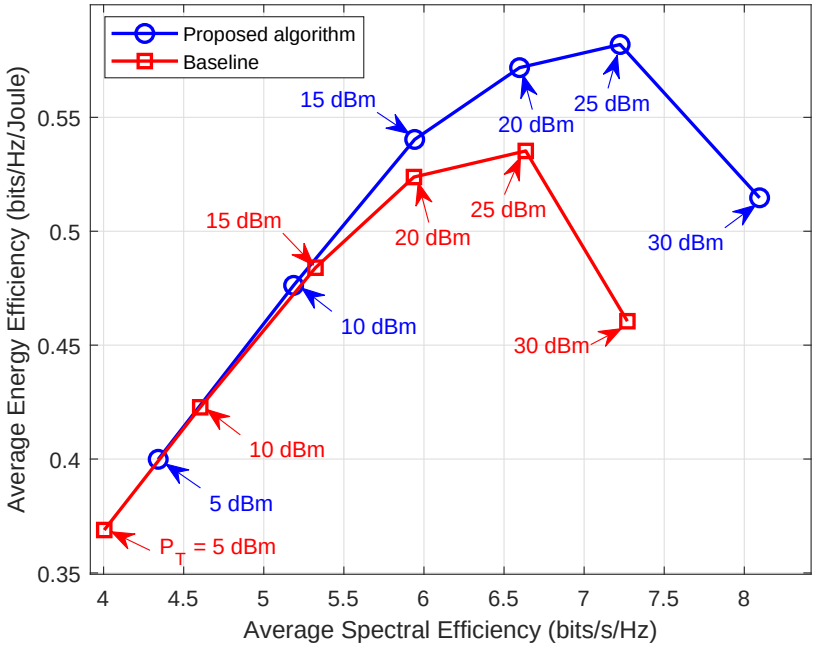

Figure 4. Average EE-SE trade-offs under proposed algorithm and baseline, with $a = 0.5$.

5. Conclusions

A RIS-aided multi-user MISO downlink system was investigated in this paper. An optimization model was used to design the transmit precoding matrix at the BS and the phase shift values at the RIS to conduct the maximization of the weighted sum of EE and SE, considering the power constraint at the BS, RIS's RC with constant modulus, and RIS's phase shifters with continuous values. We finally attained EE-SE trade-off under different circumstances by changing the value of the weight factor and got the closed-form solution of phase shift values at the RIS, while the optimal precoding matrix was obtained through the standard convex optimization algorithms. Simulations results illustrated that the presented optimization algorithm possesses fast convergence rates under different values of the power budget at the BS. It also showed that the optimization over the RC of RIS could significantly improve the EE and SE of the system.

Author Contributions: L.Y. perceived the idea. M.Z. wrote the manuscript, performed the analytic calculations, and derived the models. K.H. performed the simulations and analyzed the data. L.T. contributed to the revising and proofreading. All authors have read and agreed to the published version of the manuscript.

Funding: This work was supported in part by the Fundamental Research Funds for the Central Universities and School of Information Science and Engineering of Southeast University through Student Research Training Program.

Conflicts of Interest: The authors declare no conflict of interest.

References

1. Liaskos, C.; Nie, S.; Tsioliaridou, A.; Pitsillides, A.; Ioannidis, S.; Akyildiz, I. A New Wireless Communication Paradigm through Software-Controlled Metasurfaces. *IEEE Commun. Mag.* **2018**, *56*, 162–169. [CrossRef]
2. Ma, Y.; Shen, Y.; Yu, X.; Zhang, J.; Song, S.H.; Letaief, K.B. A Low-Complexity Algorithmic Framework for Large-Scale IRS-Assisted Wireless Systems. In Proceedings of the 2020 IEEE Globecom Workshops (GC Wkshps), Taipei, Taiwan, 7–11 December 2020; pp. 1–6.
3. Huang, C.; Hu, S.; Alexandropoulos, G.C.; Zappone, A.; Yuen, C.; Zhang, R.; Renzo, M.D.; Debbah, M. Holographic MIMO Surfaces for 6G Wireless Networks: Opportunities, Challenges, and Trends. *IEEE Wirel. Commun.* **2020**, *27*, 118–125. [CrossRef]
4. Wu, Q.; Zhang, R. Intelligent Reflecting Surface Enhanced Wireless Network via Joint Active and Passive Beamforming. *IEEE Trans. Wirel. Commun.* **2019**, *18*, 5394–5409. [CrossRef]
5. Huang, C.; Zappone, A.; Alexandropoulos, G.C.; Debbah, M.; Yuen, C. Reconfigurable Intelligent Surfaces for Energy Efficiency in Wireless Communication. *IEEE Trans. Wirel. Commun.* **2019**, *18*, 4157–4170. [CrossRef]
6. Zhou, G.; Pan, C.; Ren, H.; Wang, K.; Nallanathan, A. Intelligent Reflecting Surface Aided Multigroup Multicast MISO Communication Systems. *IEEE Trans. Signal Process.* **2020**, *68*, 3236–3251. [CrossRef]
7. Huang, C.; Mo, R.; Yuen, C. Reconfigurable Intelligent Surface Assisted Multiuser MISO Systems Exploiting Deep Reinforcement Learning. *IEEE J. Sel. Areas Commun.* **2020**, *38*, 1839–1850. [CrossRef]
8. Wu, Q.; Zhang, R. Beamforming Optimization for Wireless Network Aided by Intelligent Reflecting Surface With Discrete Phase Shifts. *IEEE Trans. Commun.* **2020**, *68*, 1838–1851. [CrossRef]
9. ElMossallamy, M.A.; Zhang, H.; Song, L.; Seddik, K.G.; Han, Z.; Li, G.Y. Reconfigurable Intelligent Surfaces for Wireless Communications: Principles, Challenges, and Opportunities. *IEEE Trans. Cogn. Commun. Netw.* **2020**, *6*, 990–1002. [CrossRef]
10. Zhang, J.; Björnson, E.; Matthaiou, M.; Ng, D.W.K.; Yang, H.; Love, D.J. Prospective Multiple Antenna Technologies for Beyond 5G. *IEEE J. Sel. Areas Commun.* **2020**, *38*, 1637–1660. [CrossRef]
11. Di Renzo, M.; Zappone, A.; Debbah, M.; Alouini, M.S.; Yuen, C.; de Rosny, J.; Tretyakov, S. Smart Radio Environments Empowered by Reconfigurable Intelligent Surfaces: How It Works, State of Research, and The Road Ahead. *IEEE J. Sel. Areas Commun.* **2020**, *38*, 2450–2525. [CrossRef]
12. Özdogan, O.; Björnson, E.; Larsson, E.G. Intelligent Reflecting Surfaces: Physics, Propagation, and Pathloss Modeling. *IEEE Wirel. Commun. Lett.* **2020**, *9*, 581–585. [CrossRef]
13. Di Renzo, M.; Danufane, F.H.; Xi, X.; de Rosny, J.; Tretyakov, S. Analytical Modeling of the Path-Loss for Reconfigurable Intelligent Surfaces—Anomalous mirror or scatterer? In Proceedings of the 2020 IEEE 21st International Workshop on Signal Processing Advances in Wireless Communications (SPAWC), Atlanta, GA, USA, 26–29 May 2020; pp. 1–5.
14. You, C.; Zheng, B.; Zhang, R. Channel Estimation and Passive Beamforming for Intelligent Reflecting Surface: Discrete Phase Shift and Progressive Refinement. *IEEE J. Sel. Areas Commun.* **2020**, *38*, 2604–2620. [CrossRef]
15. Jung, M.; Saad, W.; Jang, Y.; Kong, G.; Choi, S. Performance Analysis of Large Intelligent Surfaces (LISs): Asymptotic Data Rate and Channel Hardening Effects. *IEEE Trans. Wirel. Commun.* **2020**, *19*, 2052–2065. [CrossRef]

16. Gao, Y.; Yong, C.; Xiong, Z.; Niyato, D.; Xiao, Y.; Zhao, J. Reconfigurable Intelligent Surface for MISO Systems with Proportional Rate Constraints. In Proceedings of the ICC 2020—2020 IEEE International Conference on Communications (ICC), Dublin, Ireland, 7–11 June 2020; pp. 1–7.
17. Zou, Y.; Gong, S.; Xu, J.; Cheng, W.; Hoang, D.T.; Niyato, D. Joint Energy Beamforming and Optimization for Intelligent Reflecting Surface Enhanced Communications. In Proceedings of the 2020 IEEE Wireless Communications and Networking Conference Workshops (WCNCW), Online, 25–28 May 2020; pp. 1–6.
18. Abeywickrama, S.; Zhang, R.; Wu, Q.; Yuen, C. Intelligent Reflecting Surface: Practical Phase Shift Model and Beamforming Optimization. *IEEE Trans. Commun.* **2020**, *68*, 5849–5863. [CrossRef]
19. Yang, Z.; Shi, J.; Li, Z.; Chen, M.; Xu, W.; Shikh-Bahaei, M. Energy Efficient Rate Splitting Multiple Access (RSMA) with Reconfigurable Intelligent Surface. In Proceedings of the 2020 IEEE International Conference on Communications Workshops (ICC Workshops), Dublin, Ireland, 7–11 June 2020; pp. 1–6.
20. Xiong, J.; You, L.; Huang, Y.; Ng, D.W.K.; Wang, W.; Gao, X. Reconfigurable Intelligent Surfaces Assisted MIMO-MAC with Partial CSI. In Proceedings of the ICC 2020—2020 IEEE International Conference on Communications (ICC), Dublin, Ireland, 7–11 June 2020; pp. 1–6.
21. Tang, J.; So, D.K.; Alsusa, E.; Hamdi, K.A. Resource Efficiency: A New Paradigm on Energy Efficiency and Spectral Efficiency Tradeoff. *IEEE Trans. Wirel. Commun.* **2014**, *13*, 4656–4669. [CrossRef]
22. Mahapatra, R.; Nijsure, Y.; Kaddoum, G.; Ul Hassan, N.; Yuen, C. Energy Efficiency Tradeoff Mechanism Towards Wireless Green Communication: A Survey. *IEEE Commun. Surv. Tutor.* **2015**, *18*, 686–705. [CrossRef]
23. Pan, C.; Ren, H.; Wang, K.; Xu, W.; Elkashlan, M.; Nallanathan, A.; Hanzo, L. Multicell MIMO Communications Relying on Intelligent Reflecting Surfaces. *IEEE Trans. Wirel. Commun.* **2020**, *19*, 5218–5233. [CrossRef]
24. Zhao, M.M.; Wu, Q.; Zhao, M.J.; Zhang, R. Exploiting Amplitude Control in Intelligent Reflecting Surface Aided Wireless Communication with Imperfect CSI. *arXiv* **2020**, arXiv:2005.07002.
25. Wu, Q.; Zhang, S.; Zheng, B.; You, C.; Zhang, R. Intelligent Reflecting Surface Aided Wireless Communications: A Tutorial. *arXiv* **2020**, arXiv:2007.02759.
26. Guo, H.; Liang, Y.; Chen, J.; Larsson, E.G. Weighted Sum-Rate Maximization for Reconfigurable Intelligent Surface Aided Wireless Networks. *IEEE Trans. Wirel. Commun.* **2020**, *19*, 3064–3076. [CrossRef]
27. Zhao, M.M.; Wu, Q.; Zhao, M.J.; Zhang, R. Two-timescale Beamforming Optimization for Intelligent Reflecting Surface Enhanced Wireless Network. In Proceedings of the 2020 IEEE 11th Sensor Array and Multichannel Signal Processing Workshop (SAM), Hangzhou, China, 8–11 June 2020; pp. 1–5.
28. Wang, P.; Fang, J.; Yuan, X.; Chen, Z.; Li, H. Intelligent Reflecting Surface-Assisted Millimeter Wave Communications: Joint Active and Passive Precoding Design. *IEEE Trans. Veh. Technol.* **2020**, *69*, 14960–14973. [CrossRef]
29. Yu, X.; Xu, D.; Schober, R. MISO Wireless Communication Systems via Intelligent Reflecting Surfaces: (Invited Paper). In Proceedings of the 2019 IEEE/CIC International Conference on Communications in China (ICCC), Changchun, China, 11–13 August 2019; pp. 735–740.
30. Shen, K.; Yu, W. Fractional Programming for Communication Systems—Part I: Power Control and Beamforming. *IEEE Trans. Signal Process.* **2018**, *66*, 2616–2630. [CrossRef]
31. Shi, Q.; Razaviyayn, M.; Luo, Z.; He, C. An Iteratively Weighted MMSE Approach to Distributed Sum-Utility Maximization for a MIMO Interfering Broadcast Channel. *IEEE Trans. Signal Process.* **2011**, *59*, 4331–4340. [CrossRef]
32. Boyd, S.; Vandenberghe, L. *Convex Optimization*; Cambridge University Press: Cambridge, UK, 2004.
33. Salo, J.; Del Galdo, G.; Salmi, J.; Kyösti, P.; Milojevic, M.; Laselva, D.; Schneider, C. MATLAB implementation of the 3GPP Spatial Channel Model (3GPP TR 25.996). Available online: http://www.tkk.fi/Units/Radio/scm/ (accessed on 1 June 2005).
34. Xiong, J.; You, L.; Ng, D.W.K.; Yuen, C.; Wang, W.; Gao, X. Energy Efficiency and Spectral Efficiency Tradeoff in RIS-Aided Multiuser MIMO Uplink Systems. In Proceedings of the GLOBECOM 2020—2020 IEEE Global Communications Conference, Taipei, Taiwan, 7–11 December 2020; pp. 1–6.
35. You, L.; Xiong, J.; Ng, D.W.K.; Yuen, C.; Wang, W.; Gao, X. Energy Efficiency and Spectral Efficiency Tradeoff in RIS-Aided Multiuser MIMO Uplink Transmission. *IEEE Trans. Signal Process.* **2021**, *69*, 1407–1421. [CrossRef]